Geometrical analysis of chaotic mixing in a low Reynolds number magnetohydrodynamic quadripolar flow

J. C. Leprévost, J. R. Angilella, and J. P. Brancher
Laboratoire d'Energétique et de Mécanique Théorique et Appliquée (LEMTA), INPL-ENSEM, 2 Avenue de la Forêt de Haye, 54504, Vandoeuvre-les-Nancy, France
(Received 24 August 2000; published 20 April 2001)

A mixing device for highly viscous fluids with finite electrical conductivity is investigated theoretically. Stirring is performed by means of electromagnetic forces provided by inductor wires located outside the flow domain. The flow shows hyperbolic and elliptic singular points. Inductors are displaced in a periodic manner, leading to an efficient stretching and folding mechanism. The goodness of mixing is quantified by means of a geometrical analysis based on box-counting techniques. This analysis gives valuable information about advection of a spot of dye injected in the flow, in the limit of infinite Peclet numbers. A spatiotemporal criterion for mixing efficiency is derived, and characteristic scales are analyzed. The influence of various parameters on mixing efficiency is discussed by making use of both the geometrical analysis and Poincaré sections.

DOI: 10.1103/PhysRevE.63.056309 PACS number(s): 47.27.−i

I. INTRODUCTION

Mixing in low Reynolds numbers flows is a topic of great interest in fluid dynamics as many mixing devices involve flows where viscous forces dominate. For example, efficient mixing can be performed at low Reynolds number in cavity flows (Chien, Rising, and Ottino [1]), or in the annular region between eccentric rotating cylinders (Jeffery [2], Ballal and Rivlin [3], Aref and Balachandar [4]), or between confocal elliptic cylinders (Saatdjian and Midoux [5]). The mechanism leading to these efficient mixing properties is Lagrangian chaos. Indeed, when the trajectory of a fluid point is very sensitive to its initial position, two fluid points initially close to each other might quickly move away as time evolves, so that a spot of dye injected in such a flow is likely to spread rapidly into the whole flow domain.

The flow we consider in the present paper is divergence-free and two-dimensional. If $\psi(x,y)$ denotes the stream function, the position (x,y) of a tracer evolves according to

$$\frac{dx}{dt} = \frac{\partial \psi}{\partial y}(x,y), \tag{1}$$

$$\frac{dy}{dt} = -\frac{\partial \psi}{\partial x}(x,y), \tag{2}$$

so that the system can be described as a Hamiltonian system with one degree of freedom. Such a flow cannot provide chaos, and has very poor mixing properties. However, if the phase portrait of this Hamiltonian system displays homoclinic or heteroclinic trajectories, the flow is structurally unstable and is likely to provide chaos under temporal perturbations (Ottino [6]). In particular, this makes it possible to design efficient *time-periodic* two-dimensional mixers. Time-periodicity in various two-dimensional mixers (like cavity flow, or journal-bearing flow, or flow between confocal ellipses) is provided by moving the walls in a periodic manner. In the present work time periodicity will be achieved by inducing time-periodic electric currents in a thin layer of fluid near the boundaries (''electromagnetic skin''), so that the fluid will be stirred in a periodic manner.

In order to quantify mixing efficiency one has to define what is mixing on mathematical grounds. The following mathematical (purely topological) definition has been proposed in Ref. [6] (strong topological-theoretical mixing). One will say that a flow is a mixer if *for all subset A and B of the flow domains with nonempty interior, there exist* $T>0$ *such that for all* $t>T$:$\Phi_t(A)\cap B\neq\phi$, where $\Phi_t(\mathbf{X})$ is the position at time t of a tracer initially located at $\mathbf{X}$. This means that a spot of dye (or any passive scalar) initially placed in the continuum will cover any part of the flow domain at sufficiently long times. This definition is much weaker than definitions involving the scalar concentration. Indeed, perfect mixing requires the scalar concentration to be uniform, whereas the above definition only implies that the scalar concentration is nonzero everywhere within the flow domain. As an example, consider the sedimentation of salt in a water tank after stirring: even if the salt concentration is larger at the bottom of the tank than at the top (because of gravity effects), it is nonzero everywhere, so that it would satisfy the *topological* criterion above in spite of the low quality of mixing. However, the main advantage of this criterion is that it does not require the computation of a eulerian field (scalar concentration), and can be used from Lagrangian analysis of a set of tracers. Note that the time T in the above definition depends on A and B, and is finite if molecular diffusion is non-negligible. This definition will be used and modified in Sec. III in order to take into account the length scale of the subset B, which is clearly an important parameter to quantify the goodness of mixing. Also, the position of B is an important parameter: any zone B of the flow domain has to be reached by the dye. Finally, whatever the scale l and the position $\mathbf{x}$ of B, the time T has to be set as small as possible. This means that mixing efficiency must be quantified in terms of scale, position, and time. In the present paper we make use of box-counting techniques to derive a criterion involving scale and time. It enables to plot a ''spectrum,'' where a mixing efficiency at scale l is plotted versus l, and to estimate the time required for mixing. In the next section we

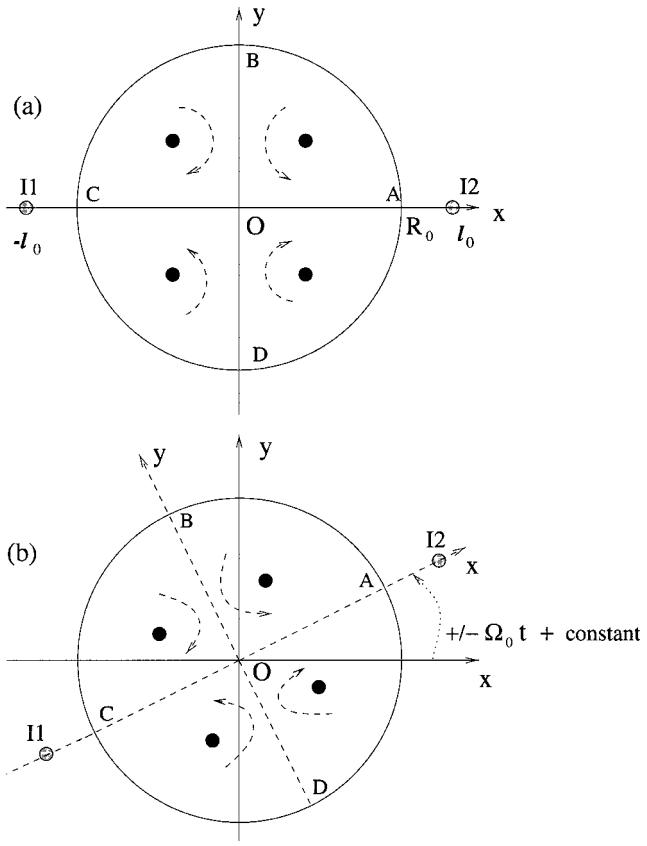

FIG. 1. Sketch of the quadripolar flow. O is a stagnation point, and the black dots (●) are the centers of four vortices of equal strength in absolute value. The flow is two-dimensional and embedded in a circle of radius R_0. (b) Shows the device after the rotation has been operated. The gray points I1 and I2 indicate the positions of the electrical inductors.

present the mixing device we use. Results are analyzed in Sec. IV.

II. THE MAGNETOHYDRODYNAMIC MIXING DEVICE

We consider an electrically conducting liquid lying within a cylindrical tank of radius R_0, and two parallel electric wires (inductors) initially located at $I_1=(l_0,0)$ and $I_2=(-l_0,0)$, with $l_0>R_0$ (Fig. 1). The electric current in inductor I_1 is $I\sqrt{2}\,\sin(\omega t)$, and electric current in inductor I_2 is $-I\sqrt{2}\,\sin(\omega t)$. The magnetic field **B** induced by these currents creates a flow within the fluid via the Laplace force. The typical velocity of this flow is proportional to I^2 and decays with l_0. When the frequency ω of the electric current is large, the induced Stokes flow can be calculated analytically (Brancher and Goichot [7]). Indeed, in this case the induced current density **j** within the fluid is located in the vicinity of the boundary $r=R_0$, where $r=\sqrt{x^2+y^2}$, inside a layer of thickness

$$\delta \sim \frac{1}{\sqrt{\mu_0 \sigma \omega}} \ll R_0, \tag{3}$$

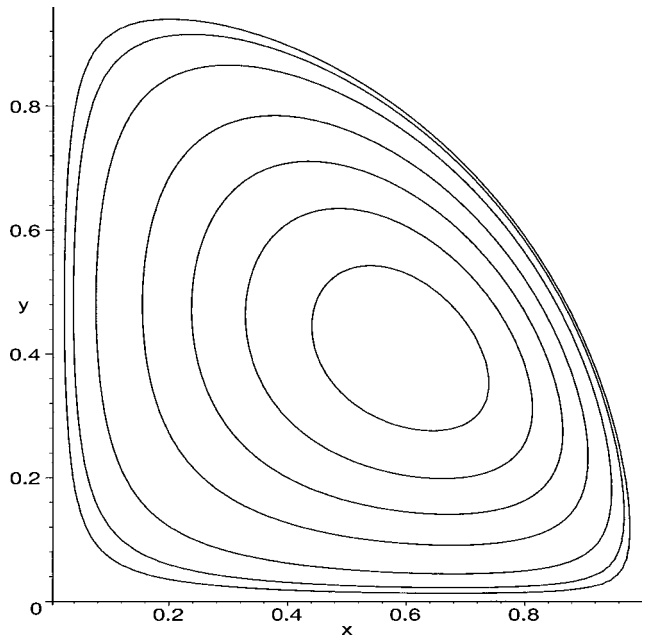

FIG. 2. Streamlines of the flow in the first quadrant obtained from the analytical solution of Ref. [7], for $d=3$.

where μ_0 denotes the magnetic permeability and σ is the electrical conductivity of the liquid. The velocity of the fluid inside the magnetic layer can then be calculated by making use of matched asymptotic expansions (Sneyd and Moffatt [8]), so that the flow inside the whole cylinder can be obtained by solving the flow equations with a boundary condition at $r=R_0$. This boundary condition reflects the dynamics, and in particular the effect of the pressure gradients created by the Laplace force, inside the magnetic layer. If u_0 denotes a typical velocity of the fluid, we assume

$$Re = \frac{u_0 R_0}{\nu} \ll 1, \tag{4}$$

where ν is the kinematic viscosity of the fluid. The flow inside the whole domain can therefore be calculated by solving the Stokes problem

$$\Delta^2 \psi = 0, \quad r < R_0, \tag{5}$$

$$\psi = 0 \quad \text{and} \quad -\frac{\partial \psi}{\partial r} = V_m(\theta) \ \text{ at } \ r = R_0, \tag{6}$$

where ψ is the stream function and $V_m(\theta)$ denotes the azimuthal velocity at $r=R_0$. This problem has been solved by Brancher and Goichot [7], and their analytical solution is used in the present paper to investigate the mixing properties of this device. The spatial structure of the resulting velocity field only depends on the ratio

$$d = \frac{l_0}{R_0},$$

which is an important parameter of the device. Figure 2

shows the streamlines of this flow when $d=3$. Heteroclinic trajectories are visible, which is an important feature for mixing.

The shape of the streamlines can be readily interpreted by means of elementary physical arguments. When the frequency ω is large the electromagnetic effects are felt only inside the layer $R_0-\delta \leqslant r \leqslant R_0$. In this layer the fluid will move from high-pressure zones to low-pressure zones. The electromagnetic pressure $B^2/2\mu_0$ has a maximum near the inductors (that is, at points A and C), and is minimum at B and D (Fig. 1). Hence, the fluid within the layer moves from A to B and D, and from C to B and D.

As mentioned above, two-dimensional steady flows have very poor mixing properties. In order to improve the mixing properties of this flow we rotate the axis I_1-I_2 with an angular velocity $\Omega(t)=\pm\Omega_0$ in a periodical manner. The sign of $\Omega(t)$ is modified every T_0 seconds, so that the stretching axis Ox (and henceforth the compression axis Oy) oscillates around its initial position [Fig. 1(b)]. The oscillation of the axes Ox and Oy leads to a stretching-and-folding mechanism, which is the purpose of our study. The Stokes numbers St satisfies

$$\mathrm{St}=\frac{R_0^2\Omega_0}{\nu}\ll 1. \tag{7}$$

Conditions (4) and (7) manifest the fact that the diffusive time scale R_0^2/ν is much smaller than both the convective time scale R_0/u_0 and the rotation time scale $1/\Omega_0$. The stretching-and-folding mechanism will be efficient if the two time scales R_0/u_0 and $1/\Omega_0$ are of the same order of magnitude, that is,

$$s=\frac{u_0}{R_0\Omega_0}\sim 1. \tag{8}$$

Clearly, this parameter is of major importance for mixing efficiency, and its influence has been investigated in details by Brancher and Goichot [7]. In the following we will take $s=1$ and discuss the effect of other parameters. Because the rotation of the axes is not steady, but reversed every T_0 seconds, it is also of interest to define the ratio:

$$k=\frac{\Omega_0 T_0}{2\pi}, \tag{9}$$

which is the number of turns performed by the axes between two consecutive reversals. This ratio is also of major importance for the quality of mixing, as it strongly influences the folding effect.

III. GEOMETRICAL TOOL TO ANALYZE MIXING EFFICIENCY

The mixing efficiency of this flow can be quantified by making use of elementary box-counting techniques (see, for example, Nicolleau [9]; Vainshtein, Sagdeev, and Rosner [10]). By following tracers (or a ''numerical spot of dye'') in the fluid (Fig. 5), one observes that the dye turns into an elongated filament, due to the stretching induced by the flow, and that this filament rapidly spreads all over the domain. Intuitively, the fact that the *spreading* is *fast* is a satisfactory criterion for efficient mixing, and in the next two sections we try to quantify these two features in terms of a *spatial* and *temporal* criterion.

A. Spatial criterion for mixing efficiency

Let $\mathcal{F}$ be the subset of the plane covered by the dye at time t. If the dye initially covers an area $\mathcal{F}_0$, then

$$\mathcal{F}=\Phi_t(\mathcal{F}_0).$$

We then quantify the space-filling properties of the dye distribution by means of elementary box-counting techniques (Falconer [11]). Let $N_0(l)$ be the minimal number of boxes of size l required to cover the flow domain. If the flow domain is a square of size L_0 we have $N_0(l)=L_0^2/l^2$, and if the flow domain is a disk of diameter L_0 we have $N_0(l)\simeq \pi L_0^2/4l^2$. In any case, we have

$$N_0(l)\sim\frac{L_0^2}{l^2}, \tag{10}$$

where L_0 is the diameter of the flow domain, and is also the size of the smallest box covering the whole domain. If $N(l,t)$ is the minimal number of boxes of size l required to cover $\mathcal{F}$ at time t, and if the dye is perfectly mixed (in the topological sense) with the carrying fluid after some time T (i.e., $\mathcal{F}$ is equivalent to the flow domain), then

$$N(l,t)=N_0(l) \quad \text{for all } l>0 \quad \text{and} \quad t>T,$$

that is, the coverage of $\mathcal{F}$ also covers the whole flow domain. This last relation manifests the fact that perfect mixing (in the geometrical sense) is achieved when the dye has a well-defined Kolomogorov capacity $D=2$, and an integral scale L_0. In the general case we have

$$N(l,t)\leqslant N_0(l),$$

so that it is interesting to consider the coverage fraction

$$\tau(l,t)=\frac{N(l,t)}{N_0(l)}, \tag{11}$$

which is equal to 1 for all $l>0$ and $t>T$ if perfect mixing is achieved, and which is smaller than 1 if not. This ratio can also be thought of as the ratio of the area of dye's coverage $[\sim l^2N(l,t)]$, to the area of the flow domain $(\sim L_0^2)$.

For a fixed time t one might have $\tau(l,t)=1$ for some scale l, $\tau(l,t)<1$ at other scales, depending on the detailed dye distribution. If we assume $\mathcal{F}$ is an elongated filament of length $\mathcal{L}(t)$ and thickness $e(t)$ (Fig. 3), the general shape of $\tau(l,t)$ can be readily obtained. Because the flow is divergence free, we have

$$\mathcal{L}(t)\sim S_0/e(t),$$

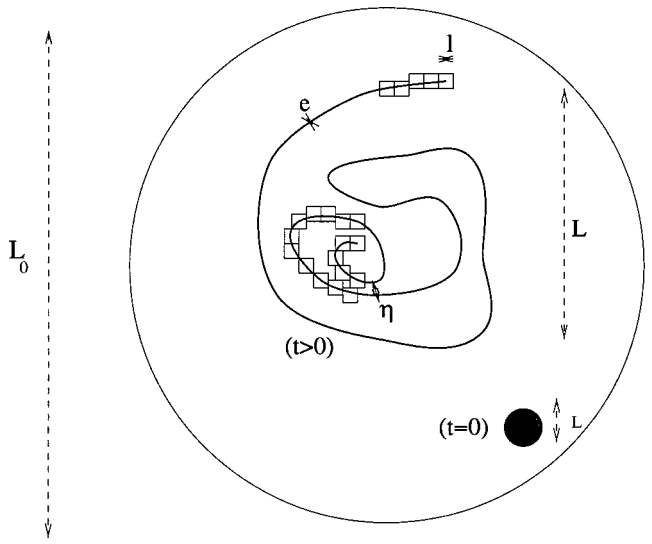

FIG. 3. Sketch of a spot of dye placed within a domain of radius R_0 at time $t=0$. For sufficiently long times the spot can be stretched into a thin filament of finite thickness e.

where S_0 is the area of $\mathcal{F}$ (which has to be constant if molecular diffusion is neglected). Also one can check that $N(l,t)$ scales like l^{-2} for scales $l \ll e(t)$ as the filament $\mathcal{F}$ is ''seen'' like a surface at those scales (Fig. 3). When l is much bigger than $e(t)$, but not too large, however, $\mathcal{F}$ can be thought of as a line, and $N(l,t)$ scales like l^{-1}. This scaling is valid up to a scale η (say), which is the scale above which the circonvolutions of the filament modify the scaling of $N(l,t)$. This scale can be thought of as the striation thickness of the dye distribution. In the general case the scaling of $N(l,t)$ for $l \gg \eta$ is unknown and depends on the detailed dynamics of the flow:

$$N(l,t) \simeq f(l) \quad \text{if} \quad \eta \ll l \ll L, \tag{12}$$

where $L=L(t)$ is the size of the smallest box covering the whole subset $\mathcal{F}$. The function $f(l)$ is unknown (and also depends on t), but decays faster than l^{-1} due to the circumvolutions of the filament. Finally, in the case where $L \ll L_0$, and when $L \ll l \ll L_0$ a single box is necessary to cover the filament, which is then seen like a ''dot,'' so that $N(l,t)=1$ there. By making use of Eq. (10), the order of magnitude of $\tau(l,t)$ can be readily obtained:

$$\tau(l,t) \sim \begin{cases} S_0/L_0^2 & \text{if } 0 < l \ll e(t) \\ \mathcal{L}l/L_0^2 & \text{if } e(t) \ll l \ll \eta(t) \\ l^2 f(l)/L_0^2 & \text{if } \eta \ll l \ll L(t) \\ l^2/L_0^2 & \text{if } L(t) \leqslant l \leqslant L_0, \end{cases} \tag{13}$$

and is sketched in Fig. 4 in log-log plot. The coverage fraction $\tau(l,t)$ quantifies the space-filling properties of the scalar distribution at a given scale l: if $\tau(l,t)$ is close to 100%, then one can say that the scalar distribution is homogeneous at scale l. Note that Eq. (10) is only an approximation when the flow domain is a disk, and could lead to $\tau(l,t)>1$ at large scales. In practice we do not use Eq. (10) [and therefore Eqs. (13)], and we compute $\tau(l,t)$ directly from Eq. (11), where both $N(l,t)$ and $N_0(l)$ are obtained by running box-counting algorithms.

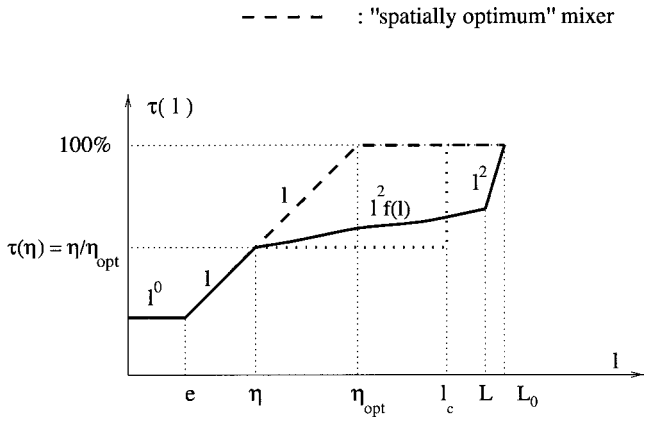

FIG. 4. Sketch of the coverage fraction $\tau(l)$ in log-log plot, in the general case (solid line), and in the case of a spatially optimum scalar distribution (dashed line). The dotted line shows $\tau(l)$ when an empty blob of size l_c is present, and mixing is spatially optimum outside this empty blob.

Because the scaling of $\tau(l,t)$ cannot be modified for $l \leqslant \eta$ (if the dye is not likely to diffuse), and also because $\tau(l,t)$ is an increasing function of l, the only way to maximize $\tau(l,t)$ for all l is to have

$$\tau(\eta,t)=1, \tag{14}$$

as shown in Fig. 4 (dashed line). In this case the spatial structure of the filament is satisfactory in that the percentage of boxes required to cover the whole domain and intersecting the filament is set as large as possible. By noticing that $eN(e,t) \sim \eta N(\eta,t) \sim \mathcal{L}$ we have

$$\tau(\eta,t) \sim \frac{\eta^2 N(\eta,t)}{L_0^2} \sim \frac{\eta}{\eta_{\text{opt}}} \leqslant 1, \tag{15}$$

where we have set $\eta_{\text{opt}}=L_0^2/\mathcal{L}$. The scale η_{opt} is the largest possible value of the striation thickness η, for a given filament length $\mathcal{L}$. Of course η_{opt} decreases with $\mathcal{L}$ and has to be as small as possible, but this is not sufficient for satisfactory mixing, as η must also be close to η_{opt} to ensure a satisfactory spatial distribution of the dye. We will therefore choose the ''spatial quality'' coefficient as the coverage fraction at scale η, that is, $\tau(\eta,t)$, which is the ratio of η to η_{opt}. Note that when $\tau(\eta,t) \sim 1$ the integral scale L satisfies $\tau(L,t) \sim 1$, that is $L \sim L_0$, which is clearly an important necessary condition for satisfactory mixing.

In the case where $f(l)$ is a power law of the form

$$f(l) \sim \left(\frac{l}{L}\right)^{-D}, \quad \eta \ll l \ll L, \tag{16}$$

with $D \in [1,2]$ then one might say that the filament has a well-defined Kolmogorov capacity D over the range of scales $[\eta,L]$. For example, when $\mathcal{F}$ is an algebraic spiral of the form $r=C\theta^{-\alpha}$, $\alpha>0$, in polar coordinates (r,θ), then

$D=1+1/(1+\alpha)$ (Vassilicos and Hunt [12]). Such a spiral can be obtained when the flow is a point vortex located at the origin, and corresponds to $D\simeq 1.67$. In general, when D is not an integer, $\mathcal{F}$ is called ''fractal.'' [Note that the Kolmogorov capacity defined above is not equivalent to the Hausdorf dimension (Falconer [11]). For example, the Hausdorf dimension of an algebraic spiral is well defined, but equals 1, whereas its Kolmogorov capacity is >1].

When Eq. (16) is satisfied, we obtain a simple expression for $\tau(\eta)$:

$$\tau(\eta)\sim \underbrace{\left(\frac{L}{L_0}\right)^2}_{\ll 1}\left(\underbrace{\frac{L}{\mathcal{L}}}_{\ll 1}\right)^{(2-D)/(D-1)}, \tag{17}$$

and we recover the fact that $\tau(\eta)$ is close to 100% only if $D\simeq 2$ and $L\sim L_0$. (Note that this result is valid only in the limit where $\mathcal{L}\gg L$, i.e., for an elongated filament.) Relation (17) can be used to estimate the efficiency of devices for which the Kolmogorov capacity D is known. For example, if we consider a fractal distribution of dye with $D=1.5$, and assuming $L\sim L_0$ and $\mathcal{L}/L=1000$ (say) then $\tau(\eta)\simeq 0.001$, so that the spatial distribution is not satisfactory. Also, the dye distribution obtained from the Baker's transformation has a Kolmogorov capacity $D=1.67$, so that it does not perfectly fulfill the above criterion. In contrast, the Archimedes spiral has a Kolmogorov capacity $D=2$, which is well defined over the range of scales $\eta\ll l\ll L$ (where η is the difference of the radii of two consecutive coils) and fulfills the spatial criterion $\tau(\eta)\sim 1$ if $L\sim L_0$. Note that the Archimedes spiral is a fictitious structure that cannot be easily obtained in a real flow.

In practice, we will not try to measure Kolmogorov capacities, and we will only measure the ratio $\tau(\eta(t),t)=\eta(t)/\eta_{\rm opt}(t)$ and check whether it is close to 1 or not.

B. Spatiotemporal criterion for mixing efficiency

A spatial criterion is not sufficient to quantify mixing efficiency, since the time required to reach a satisfactory dye distribution has to be set as small as possible. This is the reason why the temporal evolution of $\tau(\eta,t)$ is of great interest. In the following we will therefore estimate the quality of mixing by investigating the evolution of $\tau(\eta(t),t)$. If $\tau(\eta(t),t)$ increases quickly with time up to $\tau=1$, then we will say that the mixing is satisfactory. If $\tau(\eta(t),t)$ increases slowly, or stabilizes to a value $\tau\ll 1$, then we will say that the mixing is not satisfactory.

C. Characteristic scale of empty blobs

Visualizations of dye distribution often show compact areas (''empty blobs'') that are not covered by the dye, surrounded by a rather homogeneous dye distribution. This can be observed, for example, in cavity flows or journal-bearing flows when stirring is not performed in an optimum manner. Also, in journal-bearing flows, the flow domain is not simply connex, so that the diameter of the inner cylinder inevitably appears in box-counting data. The typical length of such empty blobs can be estimated as follows. We define the length scale $\kappa(t)$ where τ reaches its mean value

$$\tau(\kappa,t)=\frac{1}{L_0}\int_0^{L_0}\tau(l,t)dl. \tag{18}$$

When the dye distribution is spatially optimum, one can show that $\kappa\sim\eta_{\rm opt}$. However, when the dye distribution displays an empty blob of typical size l_c then $\tau(l)$ shows a sharp variation at $l\sim l_c$ (Fig. 4, dotted line). The above integral can then be readily calculated, and we get (removing the time variable)

$$\tau(\kappa)\sim 1+\frac{S_0 e}{2L_0^3}+\tau(\eta)\left(\frac{l_c}{L_0}-\frac{\eta}{2L_0}\right)-\frac{l_c}{L_0}, \tag{19}$$

and in the limit where $e\ll\eta\ll l_c$ and $S_0\ll L_0^2$:

$$\tau(\kappa)\sim 1+\tau(\eta)\frac{l_c}{L_0}-\frac{l_c}{L_0}. \tag{20}$$

This shows that, in this limit, we have

$$\tau(\eta)\leqslant\tau(\kappa)\leqslant 1,$$

so that the only acceptable order of magnitude for κ is

$$\kappa\sim l_c.$$

We therefore conclude that κ is of the order of $\eta_{\rm opt}$ when the spatial quality criterion is fulfilled, and is of the order of l_c if an empty blob of size l_c is present. This property is very useful to estimate the quality of mixing, and we will use it in Sec. IV.

Note that κ does not give any information about the *location* of the empty blob.

D. Link with a concentration-based criterion

Mixing efficiency is usually quantified by means of the concentration of the scalar. Because we neglect diffusion effects, the dye concentration is a binary scalar field:

$$\chi(\mathbf{x},t)$$

$$=\begin{cases}1 & \text{if } \mathbf{x}\in\mathcal{F} \qquad (21)\\ 0 & \text{otherwise,} \qquad (22)\end{cases}$$

and we define a ''weak'' concentration field:

$$c(\mathbf{x},t)=\frac{l}{l^2}\int_{\mathrm{Box}(\mathbf{x},l)}\chi(\mathbf{x},t)d^2\mathbf{x}. \tag{23}$$

Mass conservation implies

$$S_0=\int_{\text{Whole domain}}\chi(\mathbf{x},t)d^2\mathbf{x}=\sum_{i=1}^{N(l)}\int_{\mathrm{Box}(\mathbf{x}_i,l)}\chi(\mathbf{x}_i,t)d^2\mathbf{x}. \tag{24}$$

Hence we have

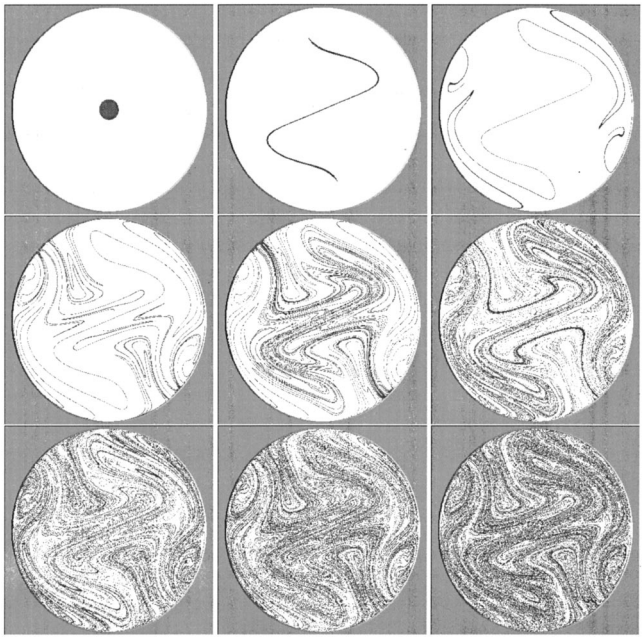

FIG. 5. Simulation of dye advection in the MHD mixer, for $d=2$, $s=1$, and $k=\frac{1}{4}$. From top to bottom and left to right: $t=0$, $t=T$, $t=2T$, $t=3T$, $t=4T$, $t=5T$, $t=6T$, $t=7T$, and $t=8T$.

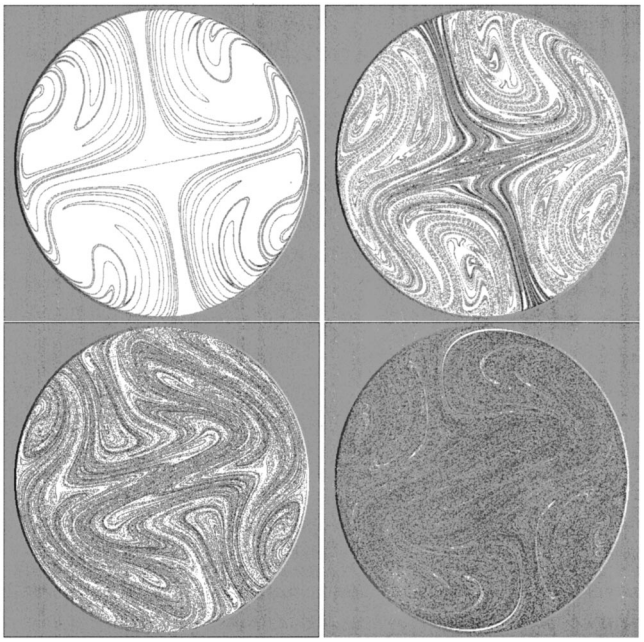

FIG. 6. Distributon of the tracers at $t=8T$, for $d=2$ and $s=1$. From top to bottom and left to right: $k=\frac{1}{16}$, $k=\frac{1}{8}$, $k=\frac{1}{4}$, and $k=\frac{1}{2}$.

$$S_0=\sum_{i=1}^{N(l)} l^2 c(\mathbf{x}_i,l), \tag{25}$$

and if $c_{\min}(l)=\min\{c(\mathbf{x}_i,l),\ i=1\ldots N(l)\}$ (which is nonzero as the minimum is taken only over boxes that intersect $\mathcal{F}$) and $c_{\max}(l)=\max\{c(\mathbf{x}_i,l),\ i=1,\ldots N(l)\}$, we get:

$$N(l)l^2 c_{\min}(l)\leqslant S_0\leqslant N(l)l^2 c_{\max}(l), \tag{26}$$

that is [since $\tau(l)=N(l)/N_0(l)\simeq l^2 N(l)/L_0^2$],

$$c_{\min}(l)\frac{L_0^2}{S}\leqslant\frac{1}{\tau(l)}\leqslant c_{\max}(l)\frac{L_0^2}{S_0}. \tag{27}$$

We therefore observe that the spatial criterion $\tau(l)=1$ is a necessary condition for the concentration $c(\mathbf{x}_i,l)$ to be uniform ($\sim S_0/L_0^2$). If, in addition, the scalar mass lying within each box is the same in every box (i.e., the scalar is ''homogeneous'' in the sense of Hentschel and Procaccia [13]), then $\tau(l)=1$ is equivalent to $c(\mathbf{x}_i,l)=S_0/L_0^2$ for all i.

The criterion based on $\tau(l)$ is therefore weaker than the concentration-based criterion, but is easier to use since it does not require the use of eulerian fields such as concentration.

E. Calculation of the scale $\eta(t)$ in the general case

In order to evaluate τ from the curve $\tau(l,t)$ we have chosen to make use of the periodicity of the mixing device. Indeed, one can check that the scalar at time t has the same ''shape'' (although it is thinner) than the scalar at time $t+T$, but displays less small-scale circonvolutions (see Fig. 5). Hence, $\tau(l,t)$ and $\tau(l,t+T)$ are very close at large scale, but also at small scale, since we know that $\tau(l,t+T)=\tau(l,t)=S_0/L_0^2$ for $l\ll e(t+T)$. It is only in the vicinity of $l=\eta$ that $\tau(l,t)$ and $\tau(l,t+T)$ differ significantly. Hence, $\tau(l,t)-\tau(l,t+T)$ displays a peak at $l\sim\eta(t)$, and the location of that peak gives us an estimation of $\eta(t)$.

IV. RESULTS

Figure 5 shows the evolution of a set of tracers in the flow. We use 5000 tracers at $t=0$, and dynamical memory allocations make it possible to use 10^6 tracers at $t=8T$. All computations have been done on a personal computer. Four simulations of this kind have been performed with $d=2$, $s=1$, and $k=\frac{1}{16}$, $k=\frac{1}{8}$, $k=\frac{1}{4}$, $k=\frac{1}{2}$. Figure 6 shows the distribution of tracers at $t=8T$ in the four cases. Significant differences exist, as large empty zones are visible in the case $k=\frac{1}{16}$ and are much smaller in the other cases. These differences can be quantified as follows.

Figures 7, 8, and 10 show the evolution of various geometrical variables for the four different simulations of scalar transport in the MHD mixer. We observe that the evolution of the perimeter of the spot (which is about twice its length $\mathcal{L}$) reflects the huge stretching properties of the flow (Fig. 7), as the perimeter increases drastically. For $k=\frac{1}{2}$, the increase of $\mathcal{L}(t)$ is faster than for the three other values of k, and its top value is also very large ($10^6\ L_0$), as stretching is more significant in this case. Note that when $k=\frac{1}{4}$ stretching is also very efficient, whereas it is much less significant for k

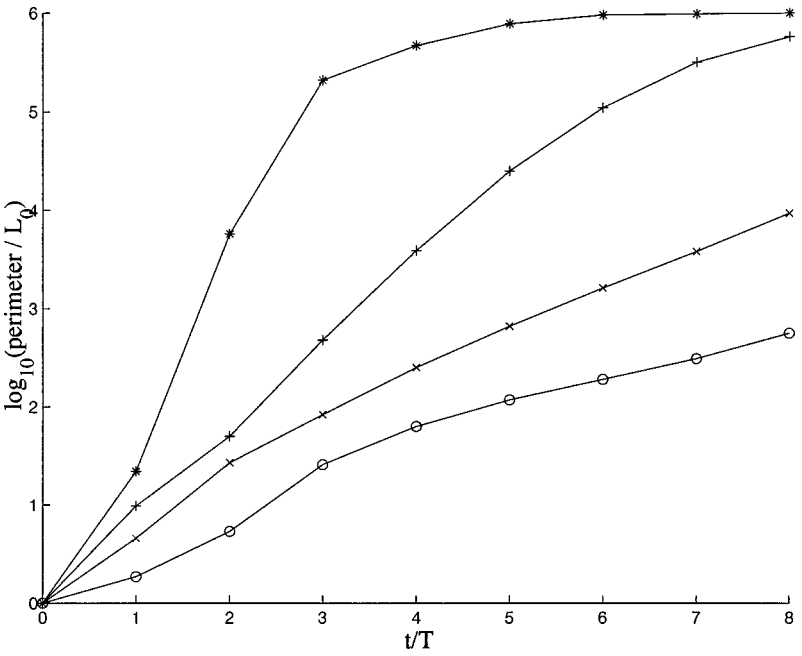

FIG. 7. Evolution of the logarithm of the perimeter (which is about twice the length $\mathcal{L}$), for $k=\frac{1}{16}$ (○), $k=\frac{1}{8}$ (×), $k=\frac{1}{4}$ (+), $k=\frac{1}{2}$ (*). In all cases $d=2$ and $s=1$.

$=\frac{1}{8}$ and $k=\frac{1}{16}$. This tendency is also visible in the evolution of the integral scale L (Fig. 8). Note that, in the four cases, the peak value of L is reached after two or three periods only, and this is a satisfactory feature for mixing efficiency. The decay of the microscale η is also very much sensitive to k. The larger the k, the faster the decay of $\eta(t)$. This tendency is also visible in Fig. 9, as the increase of $\tau(l,t)$ versus l is sharper for $k=\frac{1}{2}$ than for the three other values. However, as noticed above, it is not η alone, but the ratio $\tau(\eta)=\eta/\eta_{\mathrm{opt}}$ that enables to quantify spatial mixing efficiency. This ratio is plotted in Fig. 10, and we observe that for $k=\frac{1}{2}$ the ratio $\tau(\eta(t),t)$ versus t increases faster than for the other cases, and reaches the value 92% after seven periods. For $k=\frac{1}{4}$ the evolution of $\tau(\eta(t),t)$ is also rather satisfactory. In contrast, smaller values of k lead to a slower increase of $\tau(\eta(t),t)$. These differences confirm the tendency shown in Fig. 6.

The evolution of the scale $\kappa(t)$ gives valuable information about the spatial structure of the scalar distribution. Indeed, for $k=\frac{1}{16}$, κ remains of the order of 0.1 for long times. In contrast, for larger κ the scale κ is much smaller, and drops to 10^{-2} in the cases $k=\frac{1}{4}$ and $k=\frac{1}{2}$, in quantitative agreement with results of Fig. 6.

Poincaré sections give interesting information about mixing, and are easily obtained in the case of two-dimensional time-periodic flows [6]. Indeed, in this particular case a Poincaré section can be thought of as a set of stroboscopic images of tracers. We have computed Poincaré sections by using six tracers, the time elapsed between two consecutive images

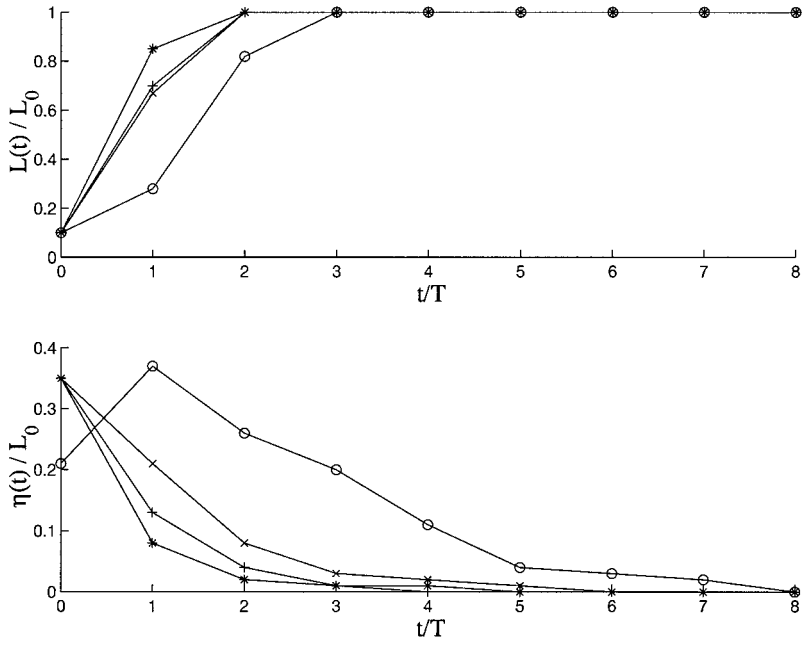

FIG. 8. Evolution of the integral scale L and of the microscale η, for $k=\frac{1}{16}$ (○), $k=\frac{1}{8}$ (×), $k=\frac{1}{4}$ (+), $k=\frac{1}{2}$ (*). In all cases $d=2$ and $s=1$.

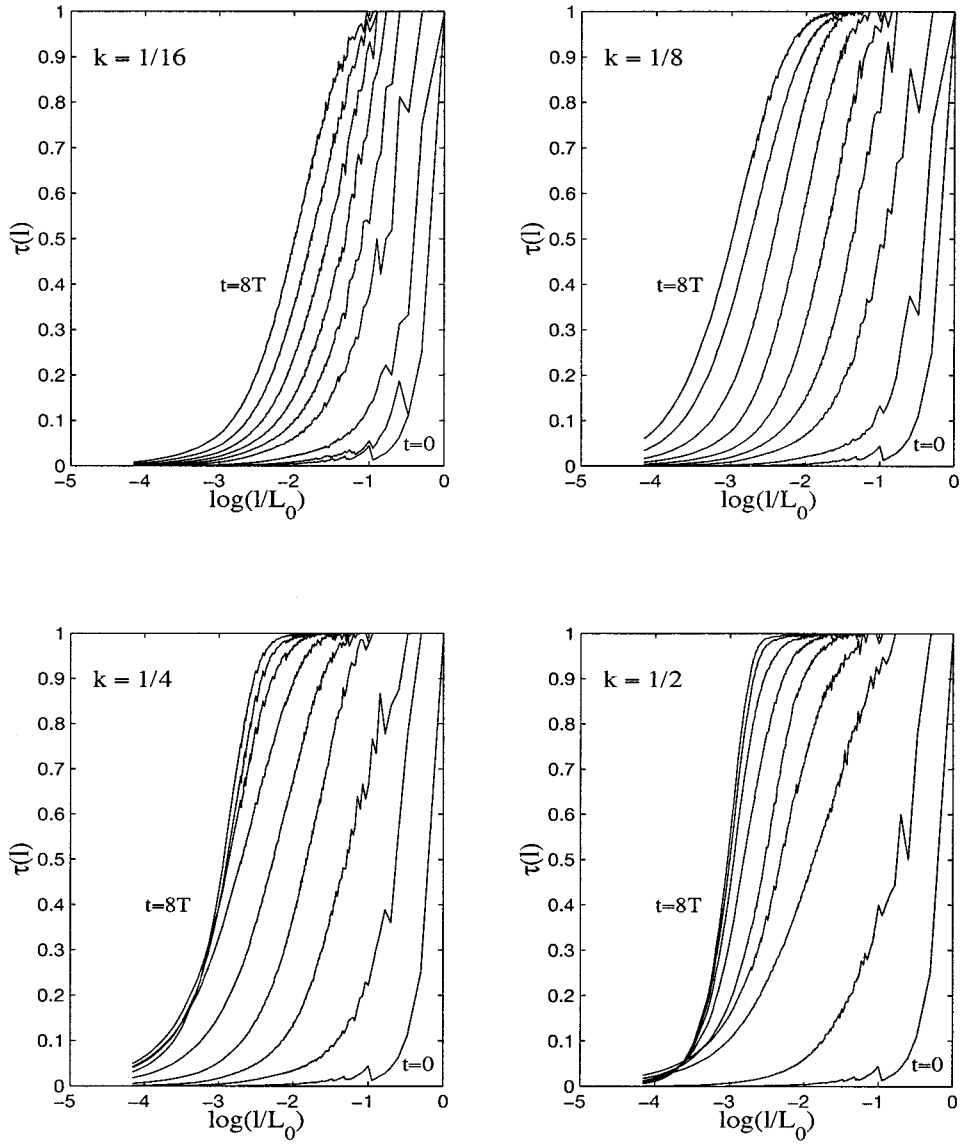

FIG. 9. Plot of the coverage fraction $\tau(l,t)$ vs l, from $t=0$ to $t=8T$ (for $d=2$, $s=1$, and four values of k).

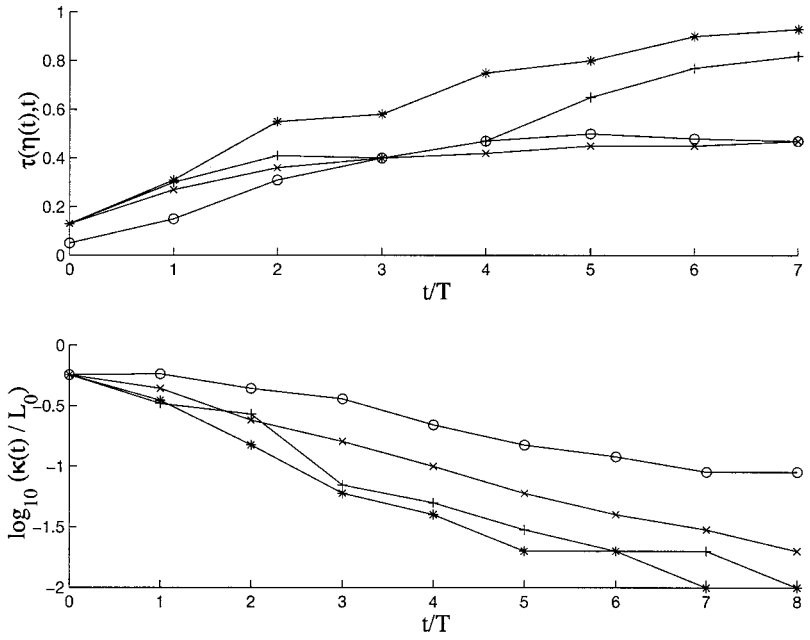

FIG. 10. Evolution of the scale κ and of $\tau(\eta)$, for $k=\frac{1}{16}$ (○), $k=\frac{1}{8}$ (×), $k=\frac{1}{4}$ (+), $k=\frac{1}{2}$ (*). In all cases $d=2$ and $s=1$.

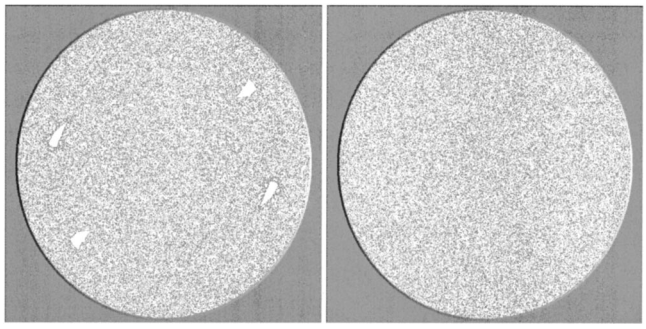

FIG. 11. Poincaré sections in the MHD mixer for $d=2$ and $s=1$, when $k=\frac{1}{16}$ (left) and $k=\frac{1}{8}$ (right). Results when $k=\frac{1}{4}$ and $k=\frac{1}{2}$ are similar to the right figure. Empty blobs of scale $\kappa\sim 0.1$ are observed in the case where $k=\frac{1}{16}$, in agreement with the geometrical analysis.

being T. Each picture of Fig. 11 shows 10 000 images. It clearly appears that the mixing device is very satisfactory in that the tracers spread in the whole flow domain, except when $k=\frac{1}{16}$. In this case four empty blobs of size about one-tenth of the cylinder diameter are visible, and this suggests that the scale $\kappa(t)$ should not drop under $0.1\,L_0$, even for long times (lower graph of Fig. 10). Other runs with large empty blobs [14] (obtained in the case $d=4$, for example) also lead to a larger limit value for $\kappa(t)$.

V. CONCLUSION

We have investigated the efficiency of mixing in a low Reynolds number MHD mixer, by making use of a topological analysis based on box-counting techniques. The main advantage of this method is that it gives quantitative, short-time information about mixing efficiency and does not require the computation of eulerian fields such as concentration. The numerical values of various geometrical parameters agree with the qualitative results plotted in Figs. 5 and 6, and also with Poincaré sections. The main drawback of the geometrical analysis is that it is based on a topological criterion for mixing goodness, which is weaker than criteria based on scalar concentration. Because the geometrical analysis is fast and can be performed directly from image-processing techniques, we believe it could be interesting to install such a tool on an experimental facility, in order to analyze and optimize mixing in real time.

The present analysis shows that the MHD mixer can be extremely satisfactory, as parameters leading to a fast and spatially efficient mixing can be found. We have fixed the time ratio $s=1$, in contrast with Ref. [7], and observed that satisfactory parameters could also be found in this case.

[1] W. L. Chien, H. Rising, and J. M. Ottino, J. Fluid Mech. **170**, 355 (1986).
[2] G. B. Jeffery, Proc. R. Soc. London, Ser. A **101**, 169 (1922).
[3] B. Ballal and R. S. Rivlin, Arch. Ration. Mech. Anal. **62**, 237 (1977).
[4] H. Aref and S. Balachandar, Phys. Fluids **29**, 3515 (1986).
[5] E. Saatdjian and N. Midoux, Phys. Fluids **6**, 3833 (1994).
[6] J. M. Ottino, *The Kinematics of Mixing: Stretching, Chaos, and Transport* (Cambridge University Press, Cambridge, England, 1989).
[7] J. P. Brancher and S. Goichot, C. R. Acad. Sci., Ser. IIb: Mec., Phys., Chim., Astron. **327**, 745 (1999).
[8] A. D. Sneyd and H. F. Moffatt, J. Fluid Mech. **117**, 45 (1982).
[9] F. Nicolleau, Phys. Fluids **8**, 2661 (1996).
[10] S. I. Vainshtein, R. Z. Sagdeev, and R. Rosner, Phys. Rev. E **56**, 1605 (1997).
[11] K. J. Falconer, *Fractal Geometry—Mathematical Foundations and Applications* (Wiley, New York, 1990).
[12] J. C. Vassilicos and J. C. R. Hunt, Proc. R. Soc. London, Ser. A **435**, 505 (1991).
[13] H. G. E. Hentschel and I. Procaccia, Physica D **8**, 435 (1983).
[14] J. C. Leprévost, Ph.D. thesis, Institut National Polytechnique de Lorraine, 2000.